Swarm and Evolutionary Computation 35 (2017) 93–110

Contents lists available at ScienceDirect

Swarm and Evolutionary Computation

journal homepage: www.elsevier.com/locate/swevo

PV cell and module efficient parameters estimation using Evaporation Rate based Water Cycle Algorithm

Dhruv Kler[1], Pallavi Sharma, Ashish Banerjee, K.P.S. Rana, Vineet Kumar

Division of Instrumentation and Control Engineering, Netaji Subhas Institute of Technology, Sector-3, Dwarka, New Delhi 110078, India

ARTICLE INFO

Keywords:
Parameter estimation
Solar cells and modules
Single diode model
Double diode model
Evaporation Rate based Water Cycle Algorithm

ABSTRACT

In order to carry out precise performance investigations and control studies on photovoltaic (PV) systems, an accurate model is always desired. In this work, a new and powerful metaheuristic optimization technique known as Evaporation Rate based Water Cycle Algorithm (ER-WCA) has been explored for effective parameters estimation of PV cell/module. Single and double diode based models of PV cell and single diode based model of PV module have been successfully identified from their respective single I-V non-linear characteristics and the modeling performance of ER-WCA, assessed in terms of root mean square error, mean absolute error and mean relative error, between computed and experimental data, is found to be superior to the several recent prominent published works particularly the modeling of a single diode based PV module. Furthermore, the PV module modeling capability of ER-WCA under varying temperature and irradiation conditions is also analysed and it is found to be effective, proving its practical applications. Based on the presented detailed investigation, it is concluded that ER-WCA is a promising optimization technique for PV cell/module identification.

1. Introduction

Inevitability of running out of fossil fuels supplemented with a global surge of power demands, calls for development of alternative renewable sources of energy. Among the various available alternative sources of renewable energy, the solar photovoltaic (PV) cell based energy sources are the most promising solutions. PV systems have shown wide acceptability due to their long life, negligible maintenance, cost effectiveness, full renewability and ease of installation. Electricity production using PV system neither produces any adverse effects such as noise and air pollution, nor does it contribute adversely towards the global warming phenomenon. A study by European Photovoltaic Industry Association (EPIA) and Greenpeace has predicted that by the year 2030 the annual reduction of CO_2, due to the usage of PV cells, to be around 1 Gton/year, which is equivalent to the emission of 300 coal plants [1]. Endorsed by these unique features, solar PV market has been on rise and from 2014 to 2015, it went up by 25% to a record 50GW, lifting the global total capacity to 227 GW. Annual market in 2015 was nearly 10 times the world's cumulative solar PV capacity, as compared to a decade earlier [2]. The efficiency, electrical power generated per unit solar energy input, of concentrator silicon solar cells is reported to be approximately 12.5% for commercially available modules [3]. To enhance the efficiency of PV systems, a control scheme is usually employed wherein an accurate modeling of a PV cell plays a key role in its performance evaluation and designing of a control scheme.

To be a winner, the proposed PV system model must be able to perfectly emulate the experimental characteristics of PV system. Over the years, considering involved physical process and associated variables, several models have been developed by researchers which have been proved to be successful to a good extent in representing the behaviour of PV systems. Amongst these two equivalent PV cell models i.e. SD based and DD based models are widely used in practice [4]. SD based model makes use of five parameters, namely, diode saturation current, photo-generated current, shunt resistance, series resistance and ideality factor while DD based model which offers higher modeling accuracy, comprises of seven parameters, namely, diode saturation currents and ideality factors for each diode, photo-generated current, shunt resistance and series resistance. Complete mathematical modeling of a PV system using the above mentioned models require estimation of aforementioned model parameters. It is worth mentioning here that these modeling parameters are not directly provided by manufactures in a data sheet form and thus require estimation from the measured non-linear I-V characteristics. A survey of prominent literature is presented below on the PV cell/module parameter estimation.

E-mail addresses: dhruvkler@gmail.com (D. Kler), pallavisharma1894@gmail.com (P. Sharma), banerjee.ashish13@gmail.com (A. Banerjee), kpsrana1@gmail.com (K.P.S. Rana), vineetkumar27@gmail.com (V. Kumar).
[1] www.nsit.ac.in.

http://dx.doi.org/10.1016/j.swevo.2017.02.005
Received 15 July 2016; Received in revised form 8 January 2017; Accepted 17 February 2017
Available online 21 February 2017

Nomenclature and abbreviations

Parameter	*description*
a	Diode Ideality Factor
a_1	Diffusion Diode Ideality Factor
a_2	Recombination Diode Ideality Factor
I_d	Diode Current (A)
I_{d1}	First Diode Current (A)
I_{d2}	Second Diode Current (A)
I_{sh}	Shunt Resistance Current (A)
I	Cell Output Current (A)
I_o	Diode Saturation Current (μA)
I_{o1}	Diffusion Current (μA)
I_{o2}	Saturation Current (μA)
I_{ph}	Photo generated Current (A)
k	Boltzmann Constant (1. 3806503 x 10^{-23} J/K)
q	Electronic Charge (1. 60217646×10^{-19} C)
R_s	Series Resistance (Ω)
R_{sh}	Shunt Resistance (Ω)

Parameter	*description*
T	Temperature of Junction (K)
G	Irradiance (W/m^2)
V_t	Junction Thermal Voltage
V	Cell Output Voltage
SD	Single Diode
DD	Double Diode
ER-WCA	Evaporation Rate based Water Cycle Algorithm
N	Number of Data Points
RMSE	Root Mean Square Error
AE	Absolute Error
RE	Relative Error
MAE	Mean Absolute Error
MRE	Mean Relative Error
NFE	Number of Function Evaluations
N_{pop}	Population Size
d_{max}	Evaporation Constant

Majorly, two different approaches have been adopted for parameter identification problem of PV systems: deterministic and heuristic [4]. In order to be correctly applied, deterministic methods, such as least squares [5,6], Lambert W-functions [7–9], and the iterative curve fitting [10,11], impose several model restrictions in terms of convexity, continuity and differentiability. It may also be noted that deterministic methods are sensitive to the initial solution and generally converge at local optima. With the development of soft computing based optimisation techniques coupled with high speed and cost effective computing power, many heuristic methods have evolved. These advanced real-world problem solvers are robust to dynamic environments while being capable of solving complex and non-linear problems with no known initial solutions [12]. Several of these have already been explored for the parameter estimation problems of PV systems. Genetic Algorithms (GA) [13,14], Particle Swarm Optimization (PSO) and Chaos Particle Swarm Optimization (CPSO) [15,16], Differential Evolution (DE), Penalty-based DE (P-DE) and Improved Adaptive Differential Evolution (IADE) [17–19], Simulated Annealing (SA) [20], Pattern Search (PS) [21], Harmony Search (HS) [22], Cuckoo Search Algorithm (CSA) [23], Artificial Bee Colony (ABC) [24], Biogeography Based Optimization Algorithm with Mutation strategies (BBO-M) [25], Cat Swarm Optimization (CSO) [26], Modified Artificial Bee Colony (MABC) [27], Generalised Opposition based Teaching Learning Based Optimization (GOTLBO) [28] and Nelder-Mead Modified Particle Swarm Optimisation (NM-MPSO) [29] have been utilized to enhance the parameter estimation accuracy for PV systems.

Each of the above mentioned optimization algorithm has its own advantages and disadvantages. GA is known to have major shortcomings like low convergence speed and degradation in case of interactive Error Functions [13]. PSO is superior to GA but generally cannot guarantee consistent results and requires a larger computational effort to effectively converge [15]. DE has a robust mutation scheme which reduces the chances of getting trapped in local optima. However, due to the differential scheme the resulting solutions have high probability of lying outside the boundary constraints. This leads to premature convergence as these “unfeasible” solutions are not passed to the next evolution [17]. SA is heavily dependent on its initial parameters, namely cooling scheme, initial temperature and relative trade-off between them. Therefore, SA is usually tedious to tune for a specific problem [20]. PS and HS possess inherent drawback of having a weak local search capability since they are not able to maintain the algorithm’s diversity which often leads to premature convergence [21,22]. CSA modified with *Lévy* walk by Yang is able to utilize the search space efficiently resulting in superior performance but the random nature of the walk sometimes leads the algorithm to out-of-bounds parameters thereby reducing the accuracy of solutions [12]. In the classical ABC, the position of the scout bee is randomly selected which reduces the effectiveness of the algorithm since it is improbable for a randomly selected bee to be close to the global optima than the cooperative search done by employed bees after iterations [27]. CSO and NM-MPSO are both effective algorithms in terms of convergence and finding global optima but these techniques require tuning of four and six parameters respectively, making the tuning of their control parameters an extremely tedious task [26,29]. BBO-M and MABC are modified versions of BBO and ABC algorithms, requiring a relatively larger population leading to reduced computational speed [25,27]. GOTLBO inculcates the strategy of opposition-based learning which greatly increases explorative ability leading to faster convergence but is not effectively able to exploit solutions and therefore might not be able to find the optimum solution.

The literature survey, presented above, clearly illustrates applications and importance of optimization algorithms in the PV cell/module parameter estimation. Till date, no single optimization algorithm has proved to be a winner in all the optimization problems and therefore there is always a need to assess the performance of any newly developed optimisation method for finding the optimum solution of a particular problem under consideration. In general, an algorithm with smaller number of user adjustable parameters, faster convergence and higher probability of converging at global optimum is termed as an efficient technique. Recently, an efficient metaheuristic algorithm Evaporation Rate based Water Cycle Algorithm (ER-WCA) has been reported by Ali et al. [30]. It is an improvisation over Water Cycle Algorithm (WCA) [31]. ER-WCA, being a population based and gradient-free algorithm possesses all the aforementioned features of a good optimisation technique. It is based on observation of water cycle process along with the concepts of evaporation rate for streams and rivers, utilised for adaptive evaporation of water. ER-WCA forces newly generated streams to search near sea using the concept of variance. It efficiently moves towards the optimal point without getting trapped in local minima. It has been demonstrated to be superior in optimizing uni-modal and multi-modal benchmark test functions over its counterparts, such as GA, Ant Colony System (ACS), Deterministic Simplex Method (SIMPSA), Stochastic Simulated Annealing Optimization (NE-SIMPSA), ABC, *Grenade Explosion Method* (GEM) and WCA. It has also been effectively used for solving constrained complex mechanical engineering benchmark problems such as pressure vessel and rolling

element bearing problems. Superiorities of ER-WCA over the other recent optimization algorithms are sufficient to claim the creditability of this technique in optimization and this very fact has motivated the authors to efficiently estimate PV system modeling parameters using ER-WCA [30].

The significant contributions of the proposed ER-WCA based non-linear PV cell/module modeling are many, and can be summarised as follows:

1. In this article, an ER-WCA based optimization technique has been proposed, tested and validated for the efficient modeling of PV cell/module.
2. PV cell/module modeling performance of ER-WCA has been fully investigated and it is found to be superior to the other recent prominent published works.
3. For the first time, the application of PV module data from System Advisor Model (SAM) has been demonstrated for the temperature and irradiation analysis of commercially available PV systems. It may be noted that SAM is a performance and financial evaluation tool developed by National Renewable Energy Laboratory (NREL) to facilitate decision making for researchers involved in the renewable energy industry.
4. A systematic approach has been devised for tuning the ER-WCA control parameters for effective parameter estimations of the PV systems.

Rest of the paper is organized as follows. After an up-to-date literature survey, on PV cell/module modeling, in Section 1, Section 2 presents brief foundations of PV cell/module parameter estimation problem. The Error Function, to be minimised using ER-WCA, for finding the optimal solutions, has also been described in this Section. Brief introduction of ER-WCA along with its flowchart is given in Section 3. Tuning process of the ER-WCA control parameters, to yield the optimum performance for modeling SD and DD based PV cell/module models, has been presented in Section 4. Using tuned ER-WCA, modeling of aforementioned two PV systems have been performed and the results have been presented in this Section along with the performance comparison with the recent reported prominent works. Furthermore, modeling results at varying environmental conditions have also been included in this Section. Finally, concluding remarks are drawn in Section 5.

2. Mathematical model of photovoltaic cell/module

Of the numerous equivalent electrical circuit models for describing the equivalent electrical circuit of a PV cell, SD based model (also called as the single diode R_p-model) and the DD based model (the two diode model) have been widely accepted and used in most of the reported literature [4,13–29]. Brief mathematical descriptions are given below for SD based modeling of a PV cell and module followed by modeling of DD based PV cell model.

2.1. Single diode based model

This section presents the SD based PV cell model followed by the SD based PV module model. Various parameters, required to model a PV cell/module non-linear I-V characteristics, have been identified so as to completely describe the respective models.

2.1.1. Single diode based model of a PV cell

In SD based model, a PV cell is considered as a current source (I_{ph}) in parallel with a rectifying diode (D), in parallel with a shunt resistance (R_{sh}), which is responsible for the leakage current, as shown in Fig. 1. The series resistance,R_s, represents ohmic losses and material resistivity at contacts [7].

Under illuminated conditions output current is given by [32]:

$$I = I_{ph} - I_d - I_{sh} \tag{1}$$

In absence of illumination the PV cell acts as a p-n junction diode and its characteristics are governed by Shockley diode equation described below.

$$I_d = I_o\left[e^{\frac{(V+IR_s)}{aV_t}} - 1\right] \tag{2}$$

where, V_t is the thermal voltage at p-n junction of diode and is given by:

$$V_t = \frac{kT}{q} \tag{3}$$

I_{sh} is obtained as:

$$I_{sh} = \left[\frac{(V + IR_s)}{R_{sh}}\right] \tag{4}$$

Substituting Eqs. (2) and (4) in Eq. (1) the PV cell output current is expressed as:

$$I = \left[I_{ph} - I_o\left[e^{\frac{(V+IR_s)}{aV_t}} - 1\right] - \frac{(V + IR_s)}{R_{sh}}\right] \tag{5}$$

Generally given by the manufacturer, the popular measured non-linear I-V characteristic is described by Eq. (5). As seen in Eq. (5), the values of five parameters, namely,I_o, I_{ph}, R_s,R_{sh}, a are required to be estimated to completely describe the SD model of a PV cell.

2.1.2. Single diode based model of PV module

A PV module comprises of a combination of series and parallel connections of cells. The I-V characteristics of a PV module making use of N_p number of parallel strings with N_s number of cells in series in a string is given by Eq. (6) [29].

$$I = \left[I_{ph}N_p - I_oN_p\left[e^{\frac{q\left(\frac{V}{N_s}+\frac{IR_s}{N_p}\right)}{akT}} - 1\right] - \frac{\frac{VN_p}{N_s} + IR_s}{R_{sh}}\right] \tag{6}$$

2.2. Double diode model of PV cell

The above described SD based model has certain inherent drawbacks, primarily due to the assumption that the diode ideality factor,a, remains constant throughout the output voltage variation range. However, diode ideality factor is a function of voltage across the device. SD model also neglects the effect of recombination at junction at low voltages (near Open Circuit VoltageV_{oc}). Therefore, at lower voltages, ideality factor is close to 2 [4]. Considering all these issues and to make the model more realistic, the current due to recombination at junction is modeled by adding a second recombination diode in parallel with the first diffusion diode leading to DD based model of the PV cell as shown in Fig. 2 [8].

During illuminated conditions, application of KCL to the circuit in Fig. 2 yields [33]:

$$I = I_{ph} - I_{d1} - I_{d2} - I_{sh} \tag{7}$$

As described for SD based model each PV cell acts as a p-n junction

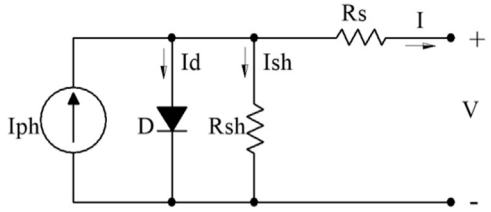

Fig. 1. Equivalent circuit of single diode model.

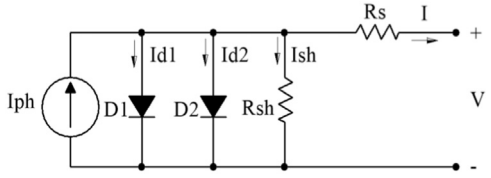

Fig. 2. Equivalent circuit of double diode model.

diode and its characteristics are governed by Shockley diode equations as described below.

$$I_{d1} = I_{o1}\left[e^{\frac{(V+IR_s)}{a_1V_t}} - 1\right] \tag{8}$$

and

$$I_{d2} = I_{o2}\left[e^{\frac{(V+IR_s)}{a_2V_t}} - 1\right] \tag{9}$$

Using KVL, one obtains shunt branch current as:

$$I_{sh} = \left[\frac{(V + IR_s)}{R_{sh}}\right] \tag{10}$$

Substituting Eqs. (8), (9) and (10) in Eq. (7), results in Eq. (11)

$$I = \left[I_{ph} - I_{o1}\left[e^{\frac{(V+IR_s)}{a_1V_t}} - 1\right] - I_{o2}\left[e^{\frac{(V+IR_s)}{a_2V_t}} - 1\right] - \frac{(V + IR_s)}{R_{sh}}\right] \tag{11}$$

As seen from Eq. (11), to completely model a PV cell characteristics using the DD model, seven parameters namely I_{o1}, I_{o2}, I_{ph}, R_s, R_{sh}, a_1, a_2 are required to be estimated.

2.3. PV system modeling: problem formulation

As mentioned above, main objective of modeling a PV cell/module is to extract optimal values of the cell/module parameters best describing the measured I-V characteristic. The characteristic equation describing the PV model is non-linear, implicit and transcendental making the PV cell/module identification an ideal candidate for optimisation. While tackling this problem using optimisation techniques one needs to define an Error Function which is to be minimised so as to lead to optimum values of the model parameters. Choice of Error Function is an important aspect as it directly affects the performance of the resulting model. In this work, the RMSE, between computed and experimental data is used as the Error Function, as defined in Eq. (12). It may be noted that RMSE is considered as the Error Function because it describes the aggregate performance of the estimated model for entire I-V characteristic as a single number [29].

$$F(\varphi) = \sqrt{\frac{1}{N}\sum_{i=1}^{N} f_i(V,\ I,\ \varphi)^2} \tag{12}$$

where N is the number of data points on the experimental I-V characteristic and the function $f_i(V, I, \varphi)$ is the difference between the experimental and estimated current values at a given point of I-V characteristic. The Error Function defined in Eq. (12), is to be minimised with respect to φ yielding the optimised model parameters. The solution vector φ represents the parameters of the model under consideration.

For SD based model, error function, $f_i(V, I, \varphi)$, and the solution vector, φ, are defined as:

$$f_i(V, I, \varphi) = \left[I - I_{ph} + I_o\left[e^{\frac{(V+IR_s)}{aV_t}} - 1\right] + \frac{(V + IR_s)}{R_{sh}}\right] \tag{13}$$

$$\varphi = \left[I_o I_{ph} R_{sh} R_s a\right] \tag{13.1}$$

Similarly, for DD based model, error function, $f_i(V, I, \varphi)$, and the solution vector, φ, are defined as:

$$f_i(V,\ I,\ \varphi) = \left[I - I_{ph} + I_{o1}\left[e^{\frac{(V+IR_s)}{a1V_t}} - 1\right] + I_{o2}\left[e^{\frac{(V+IR_s)}{a2V_t}} - 1\right] + \frac{(V + IR_s)}{R_{sh}}\right] \tag{14}$$

$$\varphi = \left[I_{o1} I_{o2} I_{ph} R_{sh} R_s a_1 a_2\right] \tag{14.1}$$

These respective Error Functions are minimised to estimate the parameters of the PV system using the ER-WCA technique described in the next section.

3. Evaporation Rate based Water Cycle Algorithm

ER-WCA is a nature inspired metaheuristic algorithm reported in 2015 for optimising continuous problems [30]. It may be noted that ER-WCA is a modified version of the WCA which was proposed in 2012 [31]. WCA is based on water cycle process and downhill movement of rivers and streams flowing to sea. ER-WCA improves on the original WCA by integrating the evaporation condition which offers two advantages: (1) Better distribution between the exploitation and exploration phases as compared to WCA and (2) Faster convergence to a global solution with accurate results than WCA. ER-WCA is implemented using four basic steps, namely initialisation, flow of streams to rivers or sea, evaporation and raining processes, and evaporation rate. These generic steps are briefly described in subsequent sub-sections.

3.1. Initialization

Due to hydrologic cycle it is assumed that rain or precipitation phenomena is constantly taking place. ER-WCA is a population based algorithm, hence "Stream" is proposed as a single solution. For an initial population of i = 1, 2,..., N_{pop} and j = 1, 2,..., N_{var} dimensional problem, a matrix of potential candidates (streams) is randomly generated between specified upper and lower bounds of parameter constraints. Each stream is an array of $1 \times N$ size.

$$\text{Stream} = [x_1, x_2, x_3 \ldots\ldots x_N] \tag{15}$$

Total population can be given as,

$$Total\ Population = \begin{bmatrix} Sea \\ River_1 \\ River_2 \\ \vdots \\ Stream_{Nsr+1} \\ Stream_{Nsr+2} \\ \vdots \\ Stream_{N_{pop}} \end{bmatrix} = \begin{bmatrix} x_1^1 & x_2^1 & \ldots x_N^1 \\ x_1^2 & x_2^2 & \ldots\ x_N^2 \\ \vdots & & \vdots\ \vdots \\ x_1^{N_{pop}} & x_2^{N_{pop}} & \ldots\ x_N^{N_{pop}} \end{bmatrix} \tag{16}$$

The cost function is used to assess the intensity (fitness) of each stream as follows;

$$\text{Cost}_i = f(x_1^i,\ x_2^i, \ldots x_N^i),\quad i = 1,\ 2,\ 3, \ldots N_{pop} \tag{17}$$

From initial population of N_{pop} streams, a number of N_{sr} are selected as sea (best fitness) and rivers (minimal fitness) among all individual streams. Also, the best individual among N_{sr} is designated as sea as shown in Eq. (18).

$$N_{sr} = Number\ of\ Rivers + 1(sea) \tag{18}$$

Rest of the population designated as streams, flowing to the rivers or sea, is calculated using Eq. (19)

$$N_{Streams} = N_{pop} - N_{sr} \tag{19}$$

Population of streams flowing to the rivers or sea is given by,

$$Population\ of\ Streams = \begin{bmatrix} Stream_1 \\ Stream_2 \\ \vdots \\ Stream_{N_{Stream}} \end{bmatrix} = \begin{bmatrix} x_1^1 & x_2^1 & \dots x_N^1 \\ x_1^2 & x_2^2 & \dots x_N^2 \\ \vdots & & \vdots \vdots \\ x_1^{N_{Stream}} & x_2^{N_{Stream}} & \dots x_N^{N_{Stream}} \end{bmatrix} \quad (20)$$

Depending on flow magnitude, sea and each river absorbs different streams and hence, varying amounts of water. Eq. (21) is used to designate streams to rivers and sea depending on intensity of flow,

$$NS_n = round\left\{ \left| \frac{C_n}{\sum_{n=1}^{N_{sr}} C_n} \right| \times N_{Streams} \right\}, \quad i = 1, 2, 3, \dots N_{sr} \quad (21)$$

where, NS_n= number of stream flows to rivers/sea.
C_n= Cost functions of sea and rivers and can be represented as Eq. (22).

$$C_n = Cost_n - Cost_{N_{sr}+1}, \quad i = 1, 2, 3, \dots N_{sr} \quad (22)$$

Since streams move towards rivers or sea, based on their flow intensity, Eq. (22) offers a convenient way to assign streams, because cost function provides a proportional way wherein more streams flow into sea than rivers. Utilizing Eq. (21) and Eq. (22), allows the best solution (sea) to control and possess more streams. Also, streams are randomly selected from among the population and one stream is assigned to one best individual only.

3.2. Flow of streams to rivers or sea

Stream generated from water eventually join each other to form new rivers and some of them may also directly flow to the sea. Finally, all streams and rivers end up in the sea (best individual). Now, the stream flow to the river along a connecting line where the distance $\vec{X}$ between them is randomly updated according to the following relation:

$$\vec{X} \in (0,\ C \times d),\ C>1, \quad (23)$$

where C is a constant whose optimum value is selected as 2 ($1 < C < 2$); $d$is the current distance between stream and river; $\vec{X}$ is a uniformly distributed random number between 0 and $(C \times d)$. Setting value of C greater than 1 allows streams to flow in different distances towards rivers and same concept can be used to describe rivers flowing to the sea. Hence for the exploitation phase, the new position for streams and rivers are given as:

$$\vec{X}_{Stream}(t+1) = \vec{X}_{Stream}(t) + rand \times C \times (\vec{X}_{River}(t) - \vec{X}_{Stream}(t)), \quad (24)$$

$$\vec{X}_{Stream}(t+1) = \vec{X}_{Stream}(t) + rand \times C \times (\vec{X}_{Sea}(t) - \vec{X}_{Stream}(t)), \quad (25)$$

$$\vec{X}_{River}(t+1) = \vec{X}_{River}(t) + rand \times C \times (\vec{X}_{Sea}(t) - \vec{X}_{River}(t)), \quad (26)$$

where *rand* is a uniformly distributed random number between 0 and 1. Eq. (24) and Eq. (25) are used for updating positions of streams flowing to rivers and sea respectively while Eq. (26) is used for updating positions of rivers which pour to the sea. If the solution obtained by a stream is better than its connecting river, the positions of river and stream are switched (i.e. stream becomes river and river becomes stream). This allows the previous river to act as a stream and the better stream (in terms of fitness) to be assigned as a new river which controls all previous streams. Similarly, improved river acts as new sea and previous sea is assigned as a new river with its own streams which were directly moving towards it. Therefore, streams related to the previous river (current updated sea) act as streams moving directly to the new sea.

3.3. Evaporation and raining processes

Evaporation and raining processes were used in the original WCA to enhance its performance. The evaporation process is similar to mutation in GA and prevents the algorithm from getting trapped in local optima. The basic concept behind this assumption is that the evaporation causes sea water to evaporate as rivers/streams flow into the sea leading to new precipitations. This concept allows the algorithm to avoid premature convergence [22]. The evaporation operator is applicable for both rivers and streams. Hence, both rivers and streams need to be checked whether they are close enough to the sea to allow the evaporation process to occur. This criterion is implemented using the following where $d_{max}$is a small number close to zero.

$$if \left| \vec{X}_{Sea} - \vec{X}^{i}_{River} \right| < d_{max}\ or\ rand<0.1,\ i=1,2,3, \dots N_{sr}-1$$

S1: *Perform raining process described by* Eq. (27)
end

After satisfying the evaporation process, the raining process is executed to form new streams in different directions. New locations of newly formed streams are generated as in Eq. (27).

$$\vec{X}^{New}_{Stream}(t+1) = \vec{LB} + rand \times (\vec{UB} - \vec{LB}) \quad (27)$$

where $\vec{LB}$ and $\vec{UB}$ are the lower and upper bounds. This criterion is also applied for streams belonging to sea.

In evaporation rate based WCA (ER-WCA), an additional raining process is also used for streams directly flowing to sea. As compared to WCA criterion S1, S2 as defined below is utilized for ER-WCA.

$$if |X_{Sea} - X^{i}_{Stream}| < d_{max}\ and\ rand < 0.1, \quad i = 1,2,3, \dots NS_1$$

S2: *Perform raining process described by* Eq. (28)
end

where Eq. (28) is given as:

$$\vec{X}^{New}_{Stream}(t+1) = \vec{X}_{new}(t) + \sqrt{\mu} \times randn(1,N) \quad (28)$$

where μdefines the searching region near sea. A larger value of μincreases the possibility for algorithm to exit from feasible region while a smaller value leads to a search in smaller region near sea. The parameter μ is set as 0.1 [30]. The term $\sqrt{\mu}$ is defined as standard deviation. Therefore, new streams with variance μ after evaporation get distributed around sea. Similarly a large value of d_{max} reduces the local search and a small value encourages the search intensity near the sea. Hence, d_{max} controls the search intensity near sea. Value of d_{max} is adaptively reduced as follows:

$$d_{max}(t+1) = d_{max}(t) - \frac{d_{max}(t)}{Max\_Iteration} \quad (29)$$

3.4. Evaporation rate for ER-WCA

Due to less streams pouring into some rivers, they have low flow and subsequently are not able to decrease their distance to sea since they get evaporated. Hence, in the modified ER-WCA, evaporation process is modified by incorporating the concept of evaporation rate. Based on designated number of streams to rivers, the Evaporation Rate (ER) is calculated as follows:

$$ER = \frac{Sum(NS_n)}{N_{sr} - 1} \times rand, \quad n = 2, \dots, N_{sr} \quad (30)$$

As seen in Eq. (30), ER is only used for streams and rivers. Also, clamorous rivers (i.e. better quality solutions) with optimum streams have lower evaporation rate, while, stagnant streams/river (i.e. worse

quality solutions) have higher ER. Hence, rivers with more designated number of streams have a lower chance of evaporating as compared to other rivers with lower number of designated/assigned streams. Furthermore, value of ER is altered iteratively which gives a stochastic nature to ER. Overall, in the ER-WCA, following two types of evaporations are introduced:

a. Evaporation used between sea and streams: pseudo-code S2 / rivers: pseudo-code S1.
b. Evaporation among rivers having few streams: pseudo-code S3.

Concept behind pseudo-code S3 is that rivers and their assigned streams having low quality solutions should be given more chances to flow to other high quality solutions, or to find better regions in terms of fitter cost function.

for i=1 : N_{sr} − 1
  if $(exp(-k/\max\_it) < rand)$ & $(NS_i < ER)$
S3: *Perform raining process described by* Eq. (27)
  end
end

where k is the iteration index. It may be noted that for evaporation among rivers, probability of evaporation is high for better quality solutions which undergo heavy explorations at early iterations and is decreased as iterations converge towards final iterations. Also, if evaporation condition is satisfied for a river, the respective river along with its streams will be evaporated (i.e. will be removed). Furthermore, new streams equal to the number of previous streams and a river is generated at new positions using Eq. (26). Fig. 3 depicts the flowchart of ER-WCA.

4. PV cell/module parameter identification: results and discussions

To assess PV cell/module estimation performance of ER-WCA a PV cell by M/S R.T.C. France and a PV module by M/S Photowatt (PWP-201) have been considered as PV system identification benchmark problems. The considered cell is a 57mm diameter commercial silicon solar cell working at 33 °C under 1 Sun (1000 W/m^2) and the considered PV module has 36 polycrystalline PV cells, connected in series, working at 45 °C, again under 1 Sun (1000 W/m^2) [34]. It may be noted that many works have used these data sets [13–29]. In this work, for estimating the cell/module parameters, reference non-linear I-V characteristics were considered as in [34]. All the simulation work, presented in this paper, made use of MATLAB® 2014b environment, working at Intel® Core™ i5 CPU, 3.2 GHz and 4 GB RAM to implement ER-WCA to identify solar cell/module parameters.

For estimating PV cell/module parameter 50 independent estimation trial runs were performed and the data for model parameters along with the fitness function for each iteration were recorded for all the case studies. Out of these 50 trials, the estimation leading to the least RMSE was considered as the final solution and has been presented as the estimation result for the respective case. To assess the robustness of the obtained solution the RMSEs of the 50 trials were statistically analysed. Additionally, the quality of the best solution and the modeling performance of ER-WCA are also assessed using Mean Absolute Error (MAE) and Mean Relative Error (MRE) as defined below, in addition to the Number of Function Evaluations (NFE).

$$Absolute\ Error\ (AE) = |I_{measured} - I_{calculated}|, \tag{31.1}$$

$$MAE = \frac{1}{N}\sum_{i=1}^{N} AE_i, \tag{31.2}$$

$$Relative\ Error\ (RE) = \left|\frac{(I_{measured} - I_{calculated})}{I_{measured}}\right|, \tag{31.3}$$

$$MRE = \frac{1}{N}\sum_{i=1}^{N} RE_i \tag{31.4}$$

where $I_{calculated}$ denotes the value of the current calculated making use of Newton's method and $I_{measured}$ denotes the experimentally obtained values of current and N being the number of data points on the I-V characteristics.

Obtained simulation results and modeling performance comparative studies of ER-WCA have been organised as follows. Out of the performed 50 trial runs the best trial leading to least RMSE is considered as the solution for which the convergence plots of Error Function along with cell parameters were recorded and have been presented. The estimated model parameters for the best trial are then tabulated followed by the resulting I-V characteristics. Relative model estimation performance comparison of ER-WCA with its most recent counterparts has also been considered and the results are presented in the form of RMSE values, since all the literature have provided this performance index. Furthermore, the MAE and MRE values have also been used for comparison in cases wherever these were reported. A notation of NA (not available) has been used where these numbers were not reported. Based on the investigation, inferences from the comparative studies are drawn and have been presented. Following sub-sections present the obtained results along with the comparative study with the potential reported literature for the respective cases.

Additionally, to assess the robustness of the obtained solutions, the RMSEs of the 50 trials were statistically analysed and have been presented using standard deviation and box plots. The standard deviation was computed for the final solutions of all the 50 trials while the box plots are used to show the robustness of ER-WCA during optimization process at few selected intermediate iterations.

4.1. Single diode based cell/module parameter identification

This section presents the parameter estimation results for the PV cell, followed by the module, using SD based model. To carry out this estimation task, upper and lower bounds for various parameters, in both the cases, i.e. cell as well as module, are listed in Table 1.

Keeping these bounds ER-WCA control parameters, namely, N_{sr} and d_{max} were tuned as described below and subsequently 50 independent estimation trial runs were carried out, and the best solution leading to least RMSE was considered as the final solution.

4.1.1. Tuning of ER-WCA control parameters

The performance of an optimisation algorithm can be greatly influenced by its control parameters. Therefore, setting of algorithm control parameters is an important task and it is an optimization problem in itself. Intrinsically, there is no explicit method, available in literature, for fine-tuning of such parameters. Researchers usually perform extensive simulations with different sets of control parameter values within their specified range. Similar approach has been employed in this work wherein intensive simulations on PV system identifications have been carried out with slight variations in the control parameters' values within a specified range, provided in the literature. In the present case, two control parameters namely N_{sr} and d_{max} were tuned to yield the best identification performances. Following is the step-by-step procedure used to find the optimal values of control parameters.

An Error Function value equivalent to value-to-reach (VTR) was defined for the identification of the control parameters of ER-WCA. For SD based model, VTR was assigned as 17.0E−4. Hence, whenever an identification trial resulted in an Error Function value below the VTR, it is classified as "acceptable" and is denoted by a green mark, otherwise marked as red. Before investigating the optimal control parameter values, effect of population size (N_{pop}) was studied by keeping N_{sr} as equivalent number of variables (i.e. 5 for SD based models) and d_{max}as 1.0E−20. The initial choice to keep d_{max} as low as

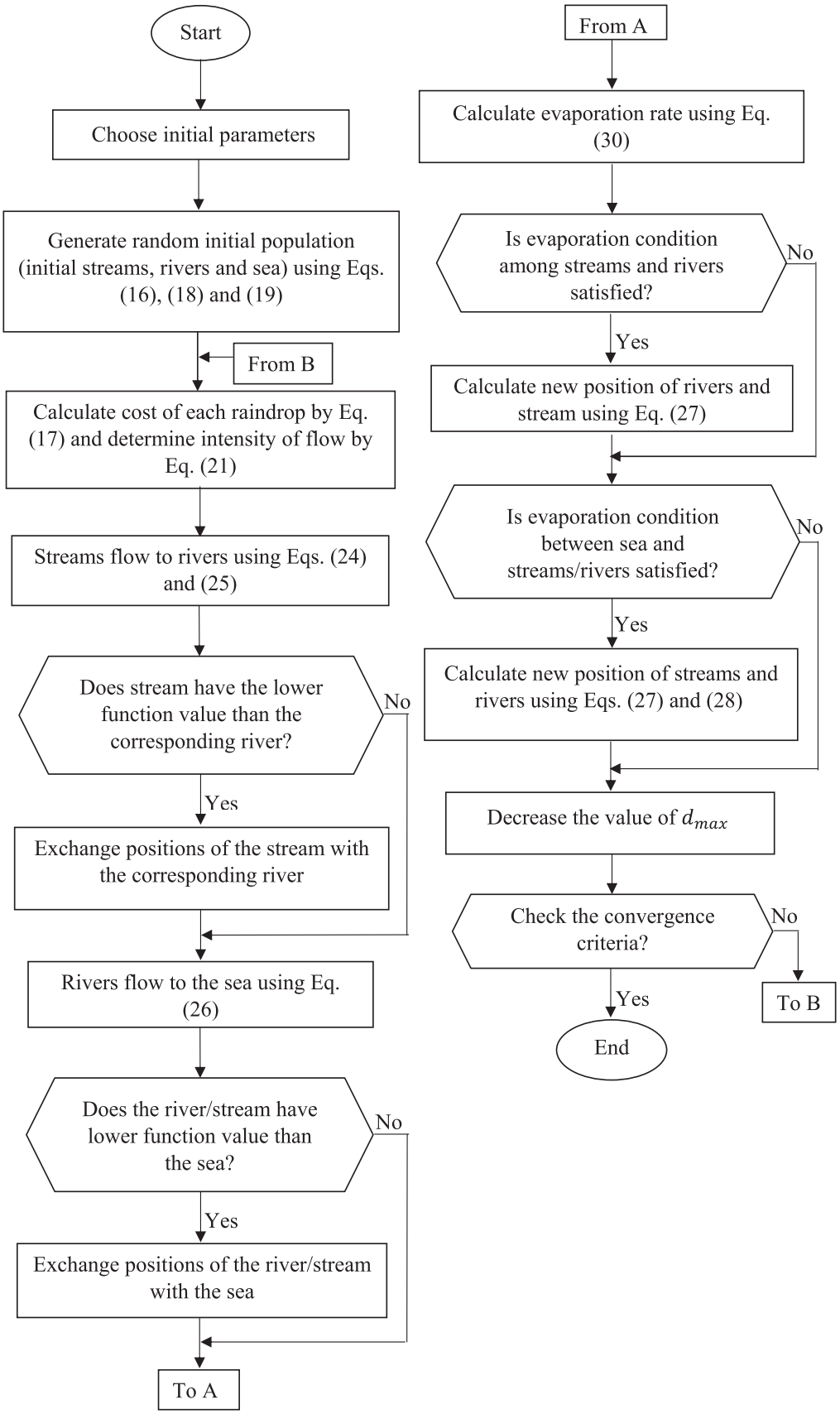

Fig. 3. Flowchart for ER-WCA.

Table 1
Parameters bounds for SD based cell/ module models.

S. No.	Parameter	Bounds for SD cell model		Bounds for SD module model	
		Lower	Upper	Lower	Upper
1.	I_o (A)	0	1E−6	0	50E−6
2.	I_{ph} (A)	0	1	0	2
3.	R_{sh} (Ω)	0	100	0	2000
4.	R_s (Ω)	0	0.5	0	2
5.	a	1	2	1	50

1.0E−20 was due to the fact that it will promote exploitation. It may be noted that ER-WCA converges very fast to its optimal solution, and therefore inherently it possesses higher exploration. This lower value of d_{max} will set a needful balance between exploitation and exploration. Now, the identification trials were conducted and Error Function values, against the measured I-V taken from [34], were recorded to find the optimal value of N_{pop}. Following are the results of SD based model identification trials.

Fig. 4(a) illustrates the value of Error Function as N_{pop} is varied from 10 to 100. It can be clearly observed that for $N_{pop} \geq 40$, Error Function is well within VTR limits while for $N_{pop} < 40$, the Error Function exceeds VTR limits. Based on these investigations the value of N_{pop} was fixed at 40. It may be noted that typically N_{pop} is kept around 8 to 10 times of the number of variables [18] and ER-WCA also follows the same. This also proves the effectiveness of ER-WCA with the ability to work well even with low population size leading to drastic increase in its computational speed.

Having fixed the value of N_{pop} as 40, next task has been to find the optimum control parameter values. For this study, N_{sr} was varied from 1 to 7 and d_{max} from 1.0E−16 to 1.0E−22, uniformly generating a total number of 49 combinations (7 × 7) of Error Function values. Fig. 4(b) shows the value of Error Function while N_{pop} is kept at 40, and N_{sr} and d_{max} are varied. It can be observed that unacceptable values of Error Function arise more frequently at the extreme combinations and, therefore, the feasible range for N_{sr} is observed from 2 to 5 while for d_{max} it is from 1.0E−18 to 1.0E−21 for SD based modeling. Based on these investigations, value of N_{sr} and d_{max} were kept as 4 and 1.0E−20, respectively.

4.1.2. Single diode based PV cell model estimation and evaluation

Fig. 5 presents the variations in Error Function, i.e. RMSE and the PV cell SD based model parameters as a function of number of iterations for the obtained best solution. As seen in Fig. 5, values of Error Function and the parameters become stable after about 100 iterations. This is as expected, because ER-WCA possesses an extraordinarily faster convergence rate. The optimum RMSE value converges to 9.8602 x 10^{-4}. It is noteworthy that though this RMSE is the same as for numerous other methods but ER-WCA attains it in less number of iterations owing to its faster convergence rate. It can also be interpreted as ER-WCA consuming lesser time to yield same identification results.

To further assess the modeling performance ER-WCA, the I-V characteristics of the considered PV cell is reproduced using the estimated SD model based cell parameters and it is compared with

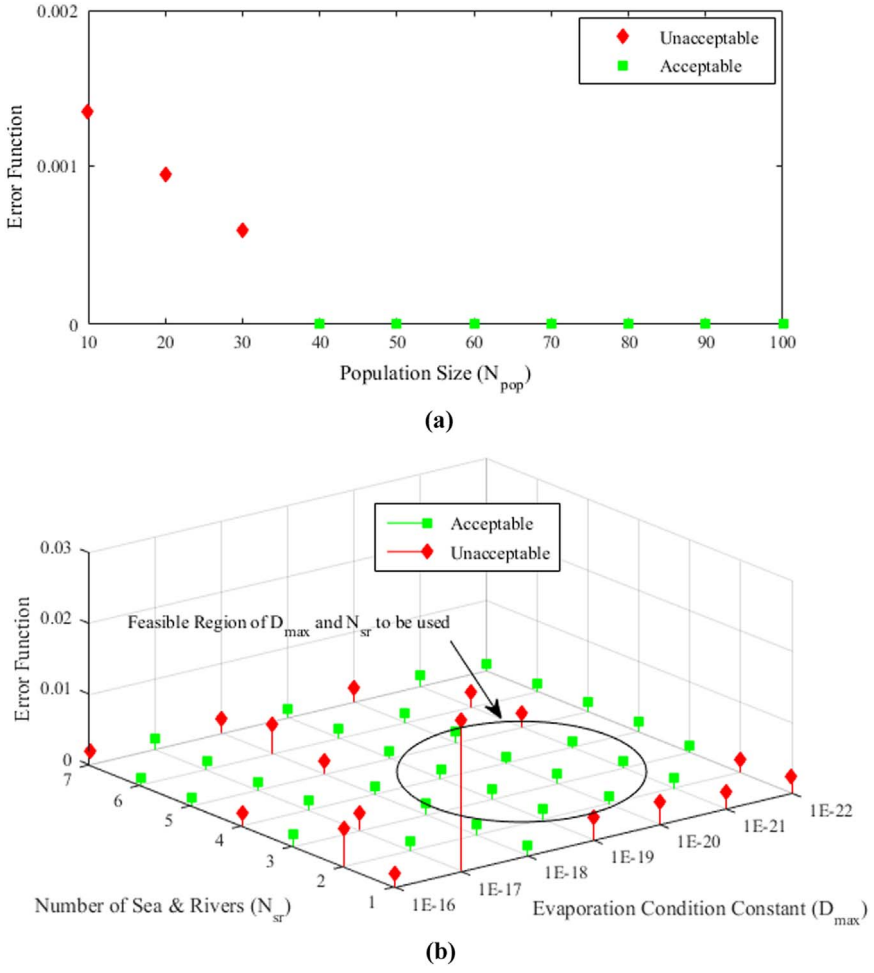

Fig. 4. Effect of control parameters on ER-WCA performance: (a) Population Size (N_{pop}); (b) Number of rivers and sea (N_{sr}) and Evaporation Condition Constant (D_{max}).

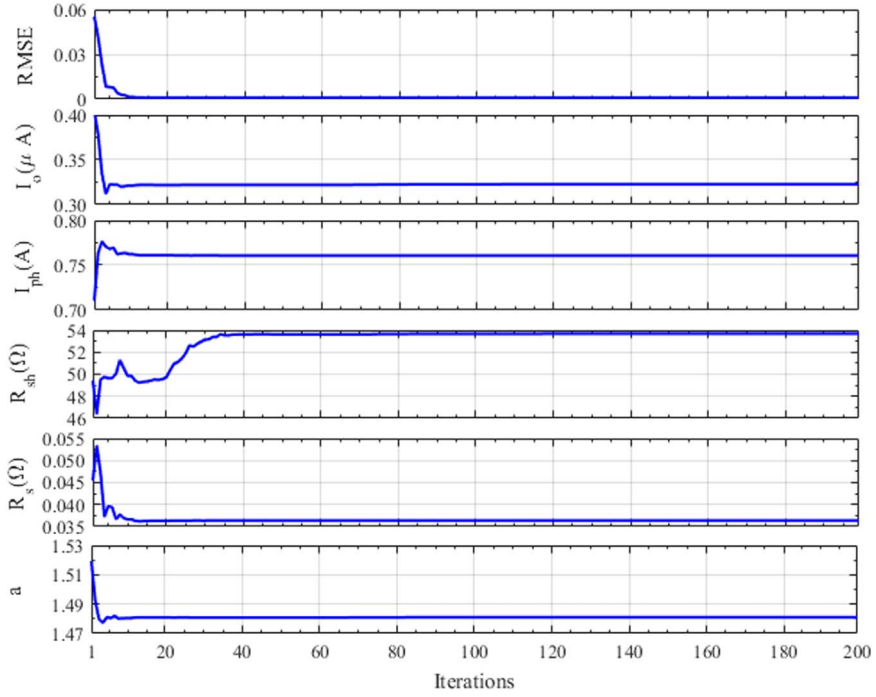

Fig. 5. RMSE and parameter profiles of the best solution for SD cell model.

the reference experimental I-V characteristics. Fig. 6 plots the experimental and computed I-V characteristics and it can be seen that the calculated values of current are in close agreement with the experimentally measured values confirming the suitability of choosing ER-WCA as an optimization technique for estimating the parameters of SD based cell model.

To further evaluate the relative SD based PV cell modeling capability of ER-WCA, its modeling results are compared with the results of recently reported seven potential literature. The performance comparison has been carried out using RMSE, MAE and MRE along with a direct comparison of NFE. Table 2 summarises the optimal SD based cell model parameters and values of RMSE, MAE, MRE and NFE, for NM-MPSO [29], GOTLBO [28], MABC [27], CSO [26], BBO-M [25], ABC [24] and IADE [19] which have also used the same PV cell. The outcome of quick convergence of ER-WCA is clearly verified in terms of number of function evaluations, which is least amongst all the considered methods. Another noteworthy outcome is the lower or same RMSE and MAE values as compared to these contemporaries, and lowest MRE amongst all the compared methods. For ease of comparison, Fig. 7 presents the RMSE values of the compared methods in a graphical form. Overall, based on these intensive simulation results, it can be concluded that for SD based PV cell modelling, ER-WCA is an effective option.

Robustness of any optimization technique is an important parameter, to assess its efficacy. For the same, RMSE values were recorded at 50th, 100th, 150th and 200th iterations over the 50 independent trial runs that were carried out for SD based cell modeling. The standard deviation, of RMSEs of final solutions, was recorded as 5.87501E−5 which is approximately an order less as compared to the best RMSE and, hence, confirming the final solutions as robust. Further for all the 50 trials the RMSEs for 50th, 100th 150th and 200th iterations were analysed using box plots as depicted in Fig. 8. As can be interpreted from Fig. 8, the size of the box plots reduces in accordance with the iterations and therefore ER-WCA possesses excellent convergence and, hence, robustness capabilities in its application towards SD based PV cell parameter estimation.

4.1.3. Single diode based PV module model estimation and evaluation

In line with presented SD based PV cell model estimation and evaluation, SD based PV module identification was also carried out for

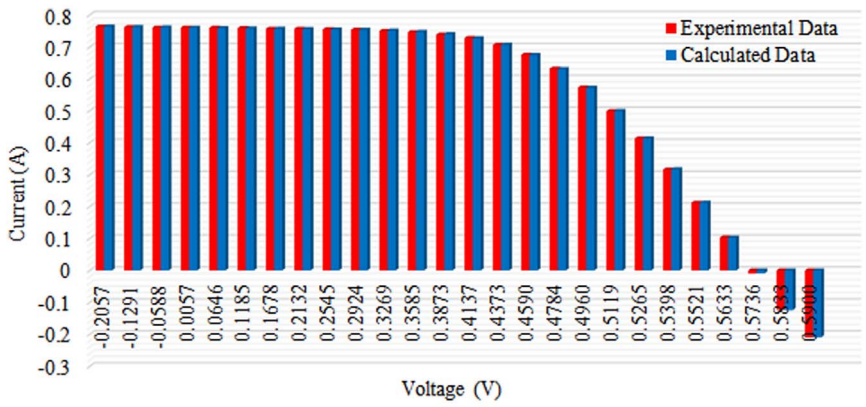

Fig. 6. I-V characteristics for SD cell model.

Table 2
Optimal parameter values and identified model performances.

Parameters	ER-WCA	NM-MPSO [29]	GOTLBO [28]	MABC [27]	CSO [26]	BBO-M [25]	ABC [24]	IADE [19]
I_o (μA)	**0.322699**	0.32306	0.331552	0.321323	0.32300	0.31874	0.3251	0.3613
I_{ph}(A)	**0.760776**	0.76078	0.76078	0.760779	0.76078	0.76078	0.7608	0.7607
R_{sh} (Ω)	**53.69100**	53.7222	54.115426	53.39999	53.7185	53.36227	53.6433	54.7643
R_s (Ω)	**0.036381**	0.03638	0.036265	0.036389	0.03638	0.3642	0.0364	0.03621
a	**1.481080**	1.4812	1.48382	1.481385	1.48118	1.47984	1.4817	1.4852
RMSE (x 10^{-4})	**9.8602**	9.8602	9.8744	9.861	9.8602	9.8634	9.8629	9.89
MAE (x 10^{-4})	**6.798546**	NA	NA	8.3118	6.7968	NA	NA	NA
MRE (x 10^{-3})	**4.543**	4.598	NA	NA	4.555	NA	8.830	NA
NFE	**8000**	350000	10000	60000	15000	NA	10000	NA

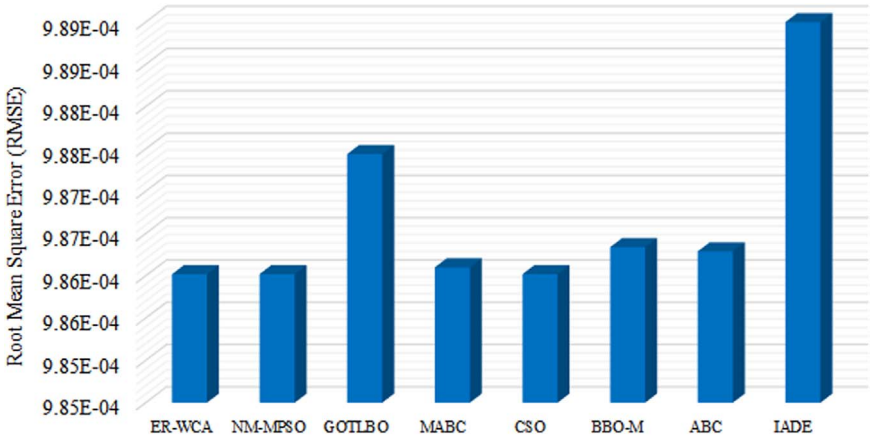

Fig. 7. RMSE based SD cell modeling performance comparison of various methods.

a module by M/S Photowatt PWP-201 [34]. The only difference has been the bounds of all the five parameters as listed in Table 1. Values of control parameters of ER-WCA were kept same as for SD based PV cell estimation. Fig. 9 presents the convergences of Error Function and the parameters of module for the obtained best solution. It can be observed, from these plots, that the values of the Error Function and the parameters become stable after about 80 iterations. This is again attributed to the unique property of quick convergence rate, of ER-WCA. An optimum value of RMSE as 0.002355 has been obtained using ER-WCA.

To further assess the PV module modeling performance of ER-WCA, I-V characteristics of the considered PV module was reproduced using the estimated parameters tabulated in Table 3. Fig. 10 shows the experimental I-V characteristic plotted against the computed ones in a graphical form wherein an accurate tracing of original module characteristic can be clearly glanced. These results clearly indicate the suitability of choosing ER-WCA as an optimization technique for estimating the parameters of SD based module model.

To carry out the relative modelling performance assessment of SD based PV module modeling capabilities of ER-WCA, its results are compared with the results of recent four potential literature, namely, NM-MPSO [29], IADE [19], SA [20] and CPSO [16], in terms of RMSE, MAE, MRE and NFE. Table 3 summarises the optimal parameter values for different methods along with the values of RMSE, MAE, MRE and NFE, as the four bases of comparison. Fig. 11 compares the RMSE values in a bar graph form for ease of demonstration. These comparisons are drawn on common grounds as these four works have also used the same PV module. From Table 3 and Fig. 11, following

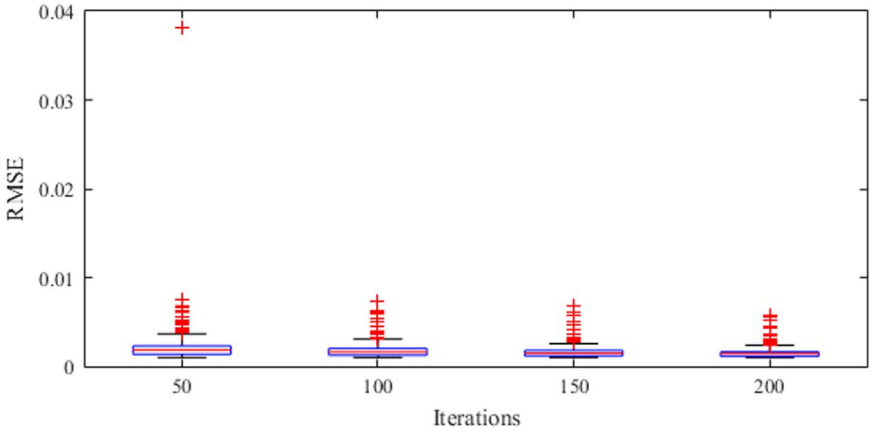

Fig. 8. Box plots of RMSEs at 50th, 100th, 150th and 200th iteration for SD cell model.

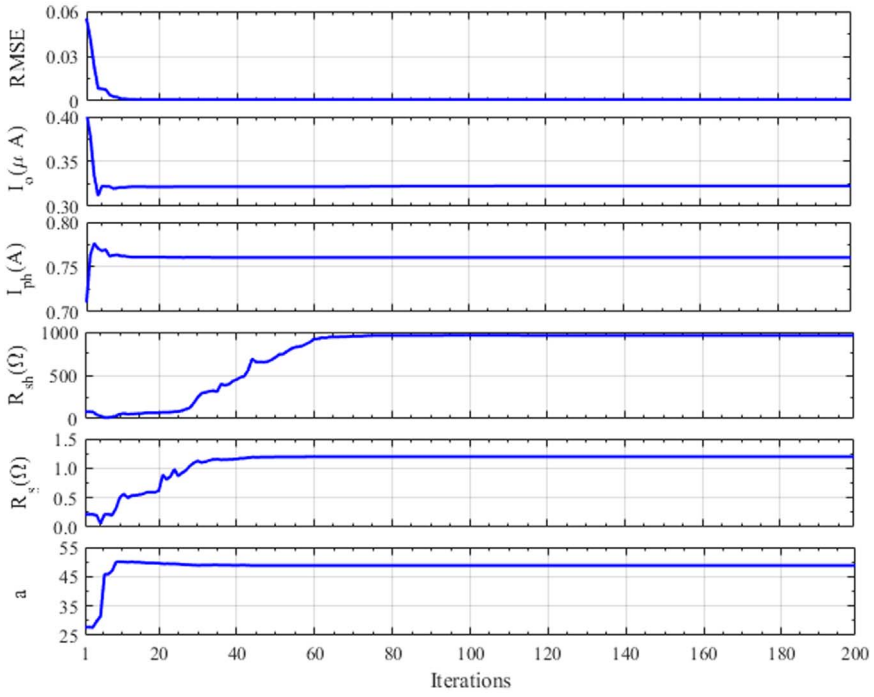

Fig. 9. RMSE and parameter values profiles of the best solution for SD module model.

Table 3
Optimal parameter values identified model performances.

Parameters	ER-WCA	NM-MPSO [29]	IADE [19]	SA [20]	CPSO [16]
I_o (μA)	**3.61455**	3.6817	3.886	3.6642	8.301
I_{ph}(A)	**1.03064**	1.0305	1.032	1.0311	1.0286
R_{sh} (Ω)	**961.053**	983.997	921.85	833.3333	1850.1
R_s (Ω)	**1.19627**	1.1944	1.189	1.1989	1.0755
a	**48.7890**	48.8598	49.068	48.8211	52.243
RMSE (x 10^{-3})	**2.3558**	2.3564	2.4	2.7	3.5
MAE (x 10^{-3})	**1.58285**	NA	NA	NA	NA
MRE (x 10^{-3})	**3.304**	3.364	NA	NA	NA
NFE	**8000**	350000	NA	NA	NA

inferences can be drawn. The main performance index, i.e. RMSE offered by ER-WCA is the least amongst the compared four methods. The MRE and NFE reported by NM-MPSO, the most recent literature, is more than that of ER-WCA. Based on these intensive investigations it can be clearly concluded that ER-WCA is a suitable optimization technique for modeling non-linear characteristic of PV module.

In line with SD based cell modeling, box plots for 50th, 100th 150th and 200th iterations, as depicted in Fig. 12, were generated using the data acquired during optimization process of 50 trial runs. As can be seen from Fig. 12, the size of the box plots reduces in accordance with the iterations and therefore ER-WCA possesses excellent convergence and robustness capabilities in its application towards SD based PV module parameter estimation. The standard deviation, of RMSEs of final solutions, was recorded to be 3.64811E−06 which is approximately three orders less as compared to the best RMSE and hence confirming ER-WCA as robust optimization technique for this application.

4.2. Double diode cell model parameter identification

First of all, control parameters were tuned for upper and lower bounds of various DD based model parameters as listed in Table 4, in line with above presented SD based modeling. For DD based model VTR was set to 1.0E−3 as it is a relatively more accurate model than SD based model. Fig. 13(a) presents the effect of N_{pop} variation on Error Function, wherein N_{pop} is varied from 20 to 100, keeping N_{sr} as equivalent number of variables (i.e. 7 for DD based model) and d_{max} as 1.0E−20. It can be clearly observed that forN_{pop} ≥50 , Error Function

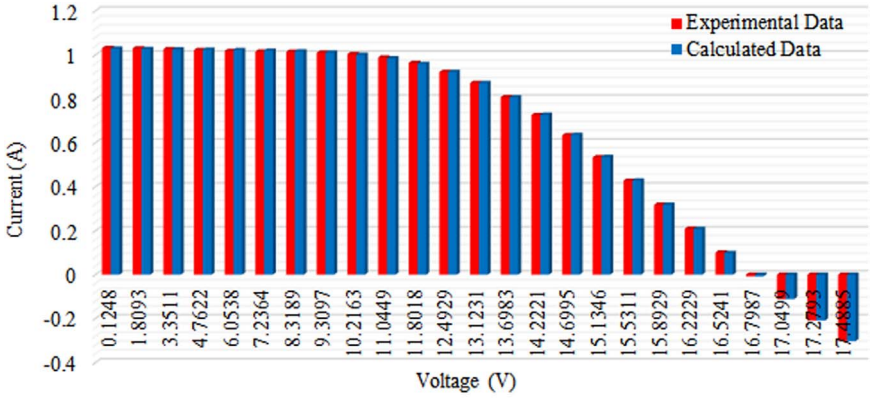

Fig. 10. I-V characteristics comparison for SD module model.

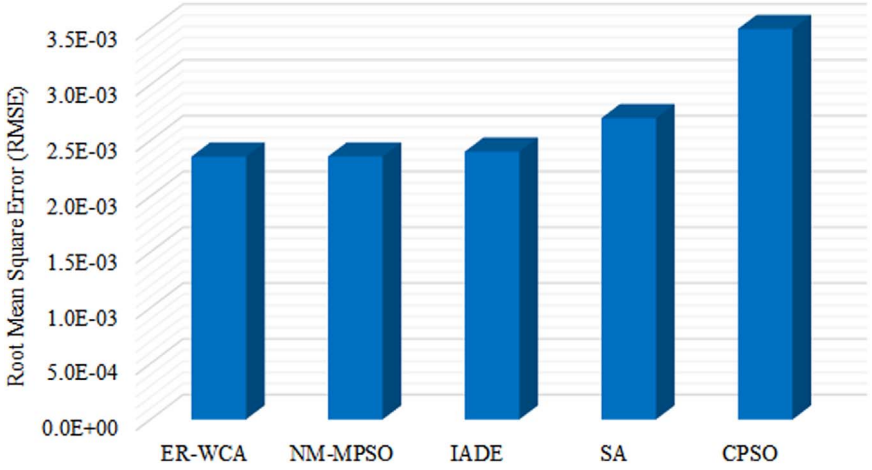

Fig. 11. RMSE based SD module modeling performance comparison of various methods.

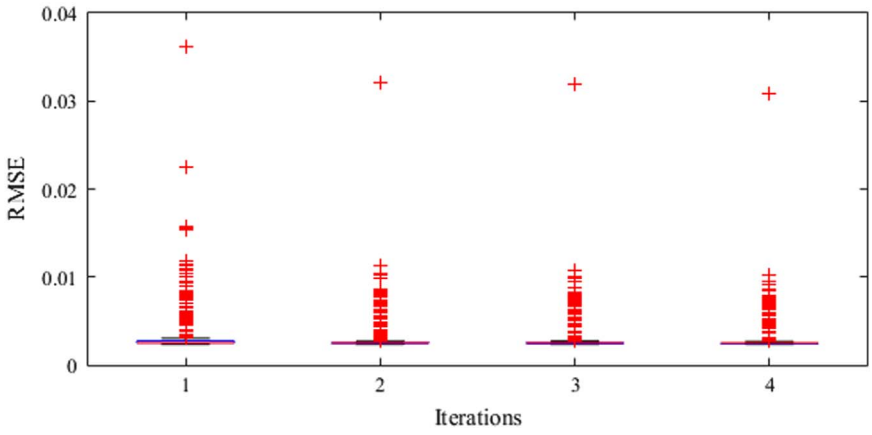

Fig. 12. Box plots of RMSEs at 50th, 100th, 150th and 200th iteration for SD module model.

is well within VTR limits while for N_{pop} <50, the Error Function exceeds VTR limits of 1.0E−3. Based on this investigation the value of N_{pop} was fixed at 50. For finding the optimum control parameter values, N_{sr} and d_{max} were again varied as in SD based modeling, generating 49 combinations (7 × 7) of Error Function. Fig. 13(b) depicts the value of Error Function while N_{pop} is kept at 50. It can be inferred that the feasible range for N_{sr} is observed from 4 to 7 while for d_{max} it is from 1.0E−19 to 1.0E−22 for DD based modeling. Based on these investigations, value of N_{sr} and d_{max} were kept as 6 and 1.0E−20, respectively.

Fig. 14 presents the variations of DD based model parameters' values and the Error Function for the obtained best solution. As seen in Fig. 14 the values of the Error Function and parameters become stable after about 40 iterations. An optimum value of 9.82484 x 10^{-4} for RMSE has been obtained using ER-WCA.

The curve fitting results of the estimated data are shown in Fig. 15 along with the measured data, wherein, it can be observed that simulated I-V characteristics obtained by ER-WCA fits experimental data to a good accuracy and confirms effectiveness of the proposed method for extraction of parameters of DD based cell model.

To further assess the relative modeling capability of ER-WCA for DD based cell model Table 5 summarises the optimal parameters and values of RMSE, MAE, MRE and NFE, the four bases of comparison made in this work, with the recent six reported works such as, NM-MPSO [29], GOTLBO [28], MABC [27], CSO [26], BBO-M [25] and ABC [24]. Fig. 16 presents the RMSE comparison in a bar chart form for convenience of observation. Table 5 depicts an extraordinary performance of ER-WCA, in terms of the least RMSE, MAE, MRE as well as NFE among the compared counterparts. Since the DD based PV cell model represents the realistic modeling of a cell this identification would be very close to the real model, while being superior to its counterparts. Based on these presented detailed results it is concluded that ER-WCA is a superior technique for DD based PV cell model identification.

Exceptional robustness and convergence capability of ER-WCA for PV DD based cell parameter estimation can be seen clearly from the box plots of RMSEs in Fig. 17 for three iterations namely 50th, 100th and 150th of RMSEs over the conducted 50 trials. The standard deviation of the final RMSEs was recorded as 1.03105E−05 which is approximately an order less as compared to the best RMSE and hence confirming the robustness.

Table 4
Parameters' bounds for DD based cell model.

S. No.	*Parameter*	*Bounds for DD cell model*	
		Lower	*Upper*
1.	I_{o1} (A)	0	1E−6
2.	I_{o2} (A)	0	1E−6
3.	I_{ph} (A)	0	1
4.	R_{sh} (Ω)	0	100
5.	R_s (Ω)	0	0.5
6.	a_1	1	2
7.	a_2	1	2

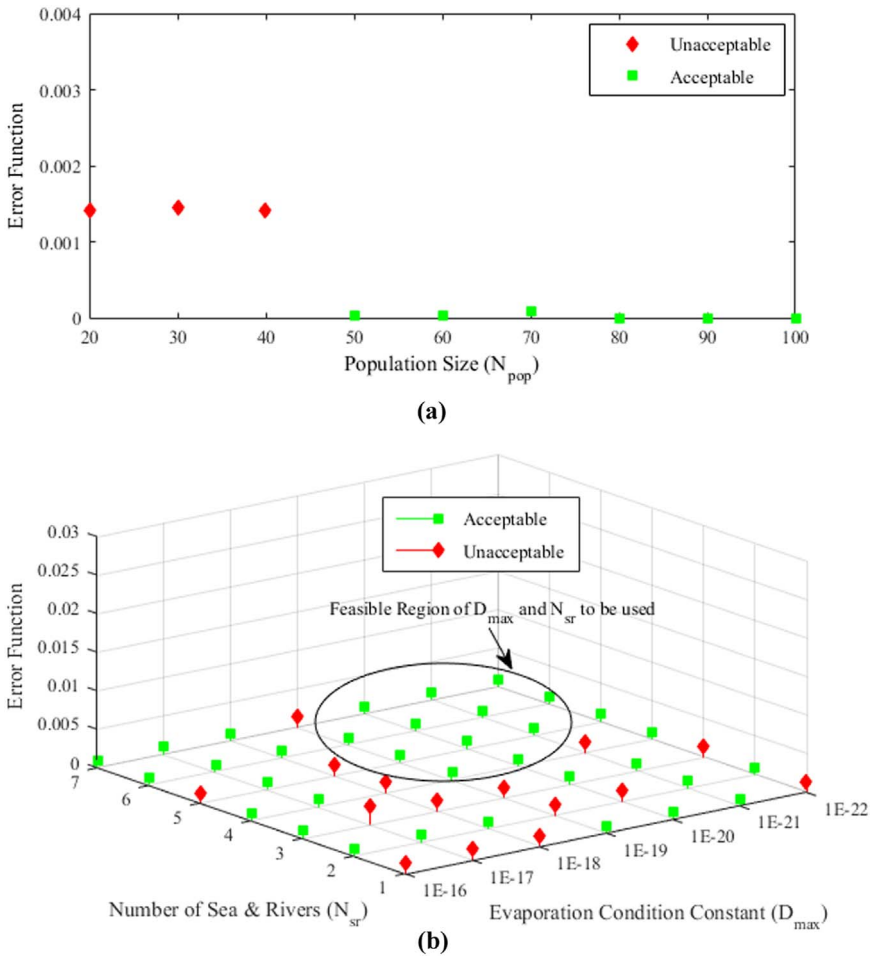

Fig. 13. Effect of control parameters on ER-WCA performance (a) Population Size (N_{pop}); (b) Number of rivers and sea (N_{sr}) and Evaporation Condition Constant (D_{max}).

4.3. ER-WCA modeling performance assessment under varying environmental conditions

In this sub-section, ER-WCA technique is used to extract parameters of SD based model for three popular PV modules, namely M/S Kyocera's KC200GT (Multi-Crystalline), M/S BP Solar's SX3200 N (Multi-Crystalline) and M/S 1Soltech's 1STH-235-WH (Mono-Crystalline). The I-V characteristics at standard temperature and irradiance conditions (STC) along with the module parameters such as Photocurrent ($I_{ph_{STC}}$), Open Circuit Voltage (V_{oc}), Reverse Saturation Current ($I_{o_{STC}}$) , Series Resistance ($R_{s_{STC}}$), Shunt Resistance ($R_{sh_{STC}}$) and temperature coefficients for Short Circuit Current (K_i) were obtained from SAM's module database [35]. Experimental I-V characteristics consisting of 41 points each, at different temperature and irradiation conditions, were computed using the above mentioned parameters of each module at STC and with the help of following equations. These equations essentially describe the linkage between the module parameters at STC and the parameters at desired temperature and irradiance [36]:

$$I_{ph} = \frac{G}{G_{STC}}\left(I_{ph_{STC}} + K_i\Delta T\right) \tag{32}$$

$$I_o = I_{o_{STC}}\left(\frac{T}{T_{STC}}\right)^3 e^{\frac{qE_g}{kn}\left(\frac{1}{T_{STC}} - \frac{1}{T}\right)} \tag{33}$$

$$R_{sh} = \frac{G_{STC}}{G}R_{sh_{STC}} \tag{34}$$

$$R_s = R_{s_{STC}} \tag{35}$$

$$V_{oc} = nV_t \ln\frac{I_{PV}}{I_o} \tag{36}$$

$$E_g = E_{g_{STC}}(1-0.0002677\Delta T) \tag{37}$$

where G and T are the irradiance and temperature values at which the module is to be modeled. Also, $E_{g_{STC}}$ is the material bandgap at STC and is stated to be at $E_{g_{STC}}$=1.12eV for silicon cells and $E_{g_{STC}}$=1.6eV for triple junction amorphous cells. The I-V characteristics, generated with the help of parameters estimated by ER-WCA, are further compared with the experimental I-V characteristics obtained from SAM [35] for the above mentioned modules at given conditions to assess the relative modeling performance of ER-WCA. Following are the modeling results of ER-WCA presented for thermal and irradiance conditions for three different modules.

4.3.1. Temperature analysis

To perform temperature analysis, three different temperature values, i.e. 25°C, 50°C and 75°C are considered at a constant irradiation (1000 W/m^2). The experimental I-V data generated at different temperatures are subsequently used for curve fitting by the proposed ER-WCA technique to estimate cell parameters and hence the I-V characteristic. The optimal parameters, extracted using ER-WCA for designated temperatures along with their RMSE performances are listed in Table 6. The corresponding estimated I-V characteristics, along with the reference ones, for the considered modules at three different temperatures are shown in Fig. 18(a) for M/S Kyocera module, Fig. 18(b) for M/S BP Solar module and Fig. 18(c) for M/S 1Soltech module. From Fig. 18 it can be inferred that the estimated characteristic curves are accurate, for the entire range, with respect to

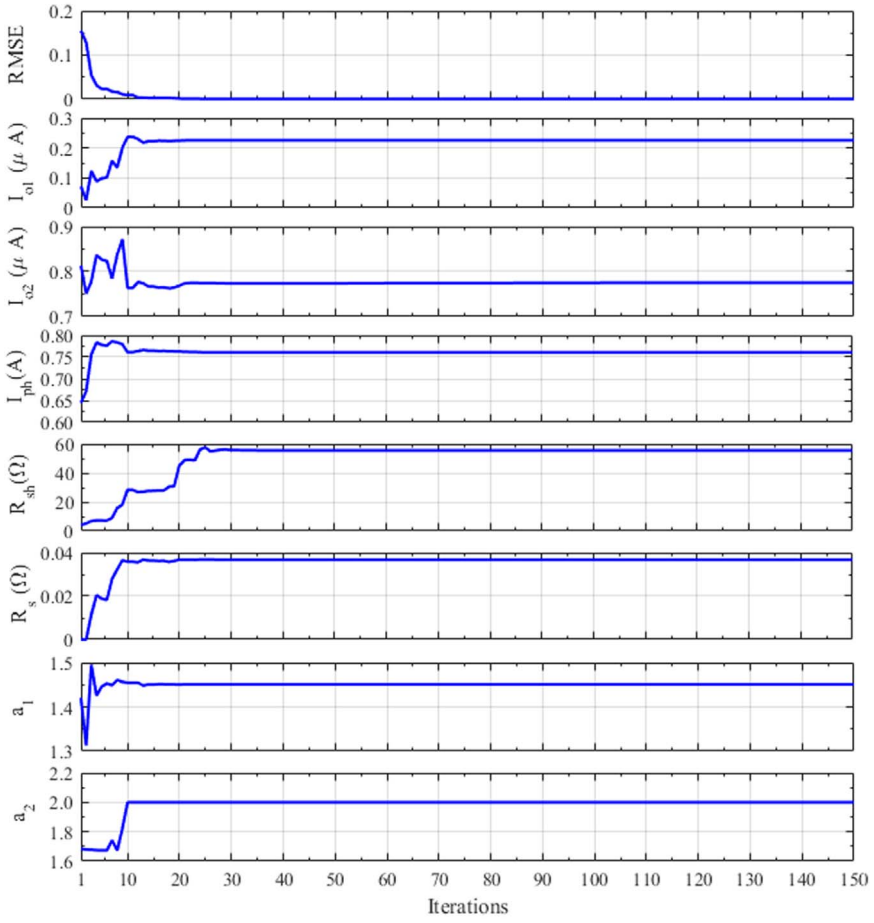

Fig. 14. RMSE and parameter values v/s iterations plot for DD cell model.

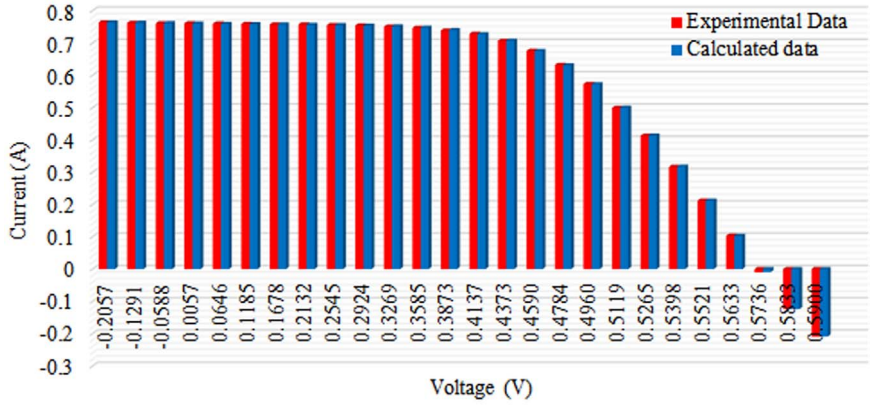

Fig. 15. I-V characteristics comparison for DD cell model.

Table 5
Optimal parameters and performance indices comparison of ER-WCA techniques and for PV using a DD cell model.

Parameters	ER-WCA	NM-MPSO [29]	GOTLBO [28]	MABC [27]	CSO [26]	BBO-M [25]	ABC [24]
I_{o1} (μA)	**0.225751**	0.22476	0.220462	0.24102992	0.22732	0.24523	0.0407
I_{o2} (μA)	**0.751019**	0.75524	0.800195	0.6306922	0.72785	0.59115	0.2874
I_{ph} (A)	**0.760781**	0.76078	0.760752	0.7607821	0.76078	0.76083	0.7608
R_{sh} (Ω)	**55.4858**	55.5296	56.075304	54.7550094	55.3813	55.0494	53.7804
R_s (Ω)	**0.0367418**	0.03675	0.036783	0.03671215	0.036737	0.03664	0.0364
a_1	**1.45093**	1.45054	1.448974	1.4568573	1.45151	1.45798	1.4495
a_2	**2.0**	1.99998	1.999973	2.0000538	1.99769	2.0	1.4885
RMSE (x 10^{-4})	**9.824849003**	9.825	9.83177	9.8276	9.8252	9.8272	9.861
MAE (x 10^{-4})	**6.65194**	NA	NA	8.2033	6.6682	NA	NA
MRE (x 10^{-3})	**4.381**	4.485	NA	NA	4.445	NA	8.2918
NFE	**7500**	350000	20000	120000	15000	NA	1500000

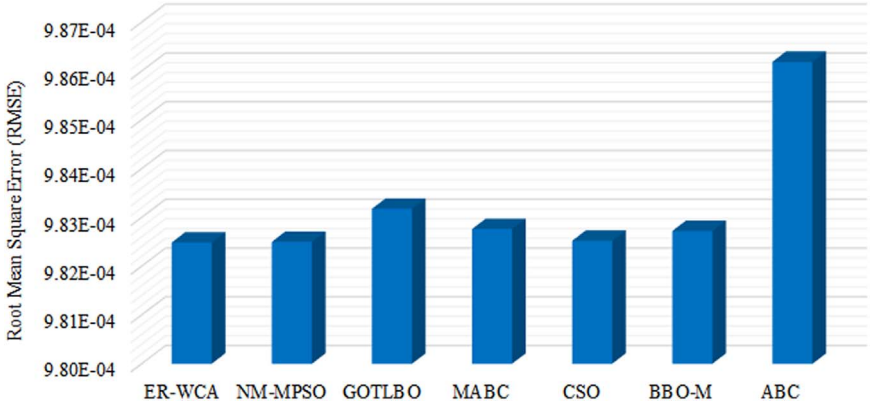

Fig. 16. RMSE based DD cell modeling performance comparison of various methods.

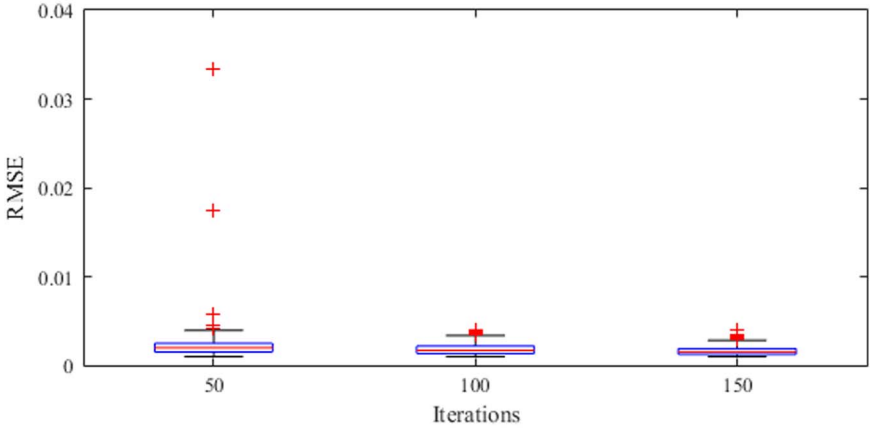

Fig. 17. Box plots of RMSEs at 50th, 100th and 150th iteration for DD cell model.

Table 6
Estimated Parameters by ER-WCA for different PV modules at three different temperature at a constant irradiance level of 1000 W/m^2.

Parameter	KC200GT	SX3200N	1STH-235-WH
T=25°C			
I_o (A)	9.810012E−10	3.968278E−8	1.409086E−9
I_{ph} (A)	8.224098	8.928015	8.539840
R_{sh} (Ω)	176.6210	658.1050	1711.843
R_s (Ω)	0.322483	0.296227	0.380653
a	1.078098	1.061789	1.065534
RMSE	17.83941E−4	5.159179E−4	18.08086E−4
T=50°C			
I_o (A)	2.423838E−8	1.130828E−6	3.788074E−8
I_{ph} (A)	8.350166	9.153585	8.716822
R_{sh} (Ω)	173.7896	631.7383	1448.942
R_s (Ω)	0.324243	0.296689	0.381773
a	1.071304	1.059620	1.061176
RMSE	5.492161E−4	6.554441E−5	8.925824E−4
T=75°C			
I_o (A)	4.027546E−7	2.019448E−5	5.961065E−7
I_{ph} (A)	8.475841	9.378331	8.894044
R_{sh} (Ω)	172.1787	647.9781	1112.303
R_s (Ω)	0.324869	0.296635	0.383962
a	1.068961	1.059910	1.053605
RMSE	9.839339E−5	1.465678E−4	6.832381E−4

Table 7
Parameters estimated by ER-WCA for three PV modules at three irradiance levels and constant temperature of 25°C.

Parameter	KC200GT	SX3200N	1STH-235-WH
G=1000 W/m^2			
I_o (A)	9.810012E−10	3.968278E−8	1.409086E−9
I_{ph} (A)	8.224098	8.928015	8.539840
R_{sh} (Ω)	176.6210	658.1050	1711.843
R_s (Ω)	0.322483	0.296227	0.380653
a	1.078098	1.061789	1.065534
RMSE	17.83941E−4	5.159179E−4	18.08086E−4
G=600 W/m^2			
I_o (A)	9.252733E−10	4.083109E−8	1.159560E−9
I_{ph} (A)	4.934781	5.356718	5.125839
R_{sh} (Ω)	292.0804	1123.254	2080.076
R_s (Ω)	0.321917	0.295242	0.383198
a	1.075513	1.063468	1.056429
RMSE	7.678673E−4	5.104184E−4	4.987503E−5
G=200 W/m^2			
I_o (A)	8.692462E−10	3.828281E−8	1.204909E−9
I_{ph} (A)	1.645074	1.785744	1.708519
R_{sh} (Ω)	868.3201	3159.954	6517.976
R_s (Ω)	0.319368	0.296319	0.380913
a	1.072741	1.059864	1.058323
RMSE	1.506510E−4	3.284413E−5	5.954443E−5

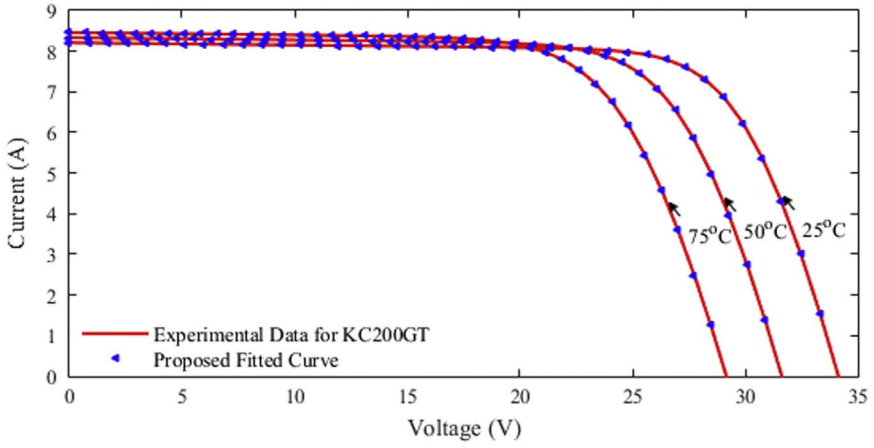

(a)

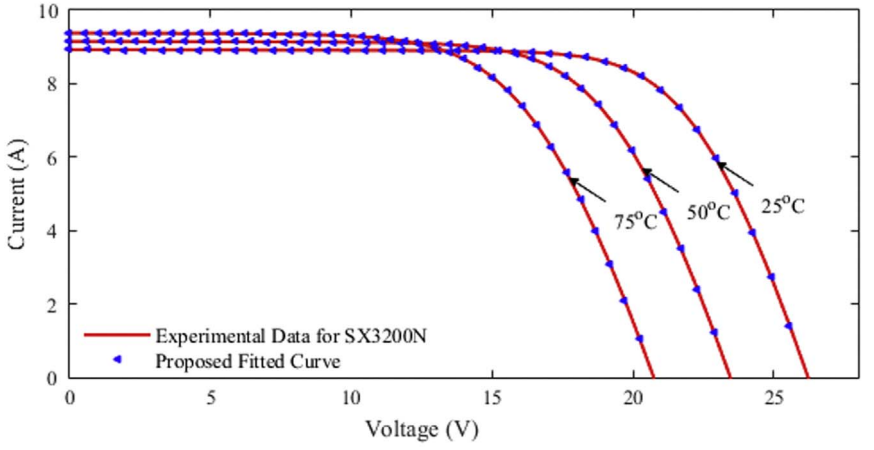

(b)

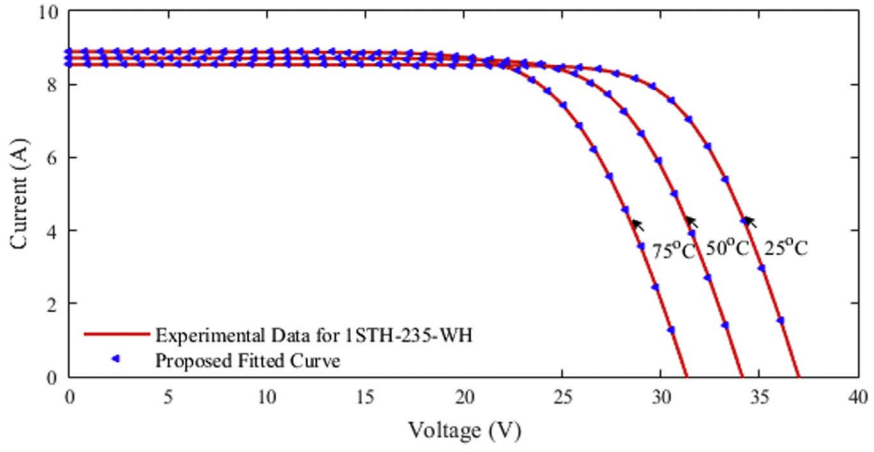

(c)

Fig. 18. Experimental and estimated I-V characteristics of PV modules at different temperatures: (a) KC200GT (b) SX3200N (c) 1STH-235-WH.

the experimental characteristics for all the three considered temperature values. A significantly low error between calculated and experimental values at all the considered temperature values is a crucial aspect of addressing two main aspects of PV system modeling: Inverter Design [37] and Photovoltaic Thermal (PVT) Efficiency [38].

4.3.2. Irradiation analysis

In line with temperature analysis, three irradiation values, i.e. 200 W/m^2, 600 W/m^2 and 1000 W/m^2 are considered for the purpose of irradiance analysis at a constant temperature (25°C). The experimental I-V characteristics were generated for these three different irradiance values using Eqs. ((32)–(37)) which were further used as the reference values for parameter estimation by ER-WCA. Table 7 list the extracted model parameters along with the obtained RMSEs of the three modules at considered three different irradiation conditions. In Table 7, low RMSE values effectively validate the accuracy of ER-WCA under varying irradiation conditions. Furthermore, using the extracted parameters, I-V characteristics for considered three modules at three

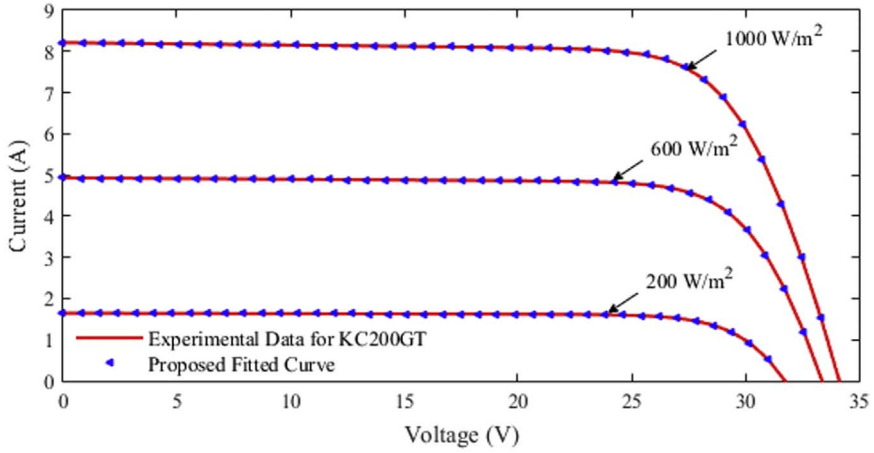

(a)

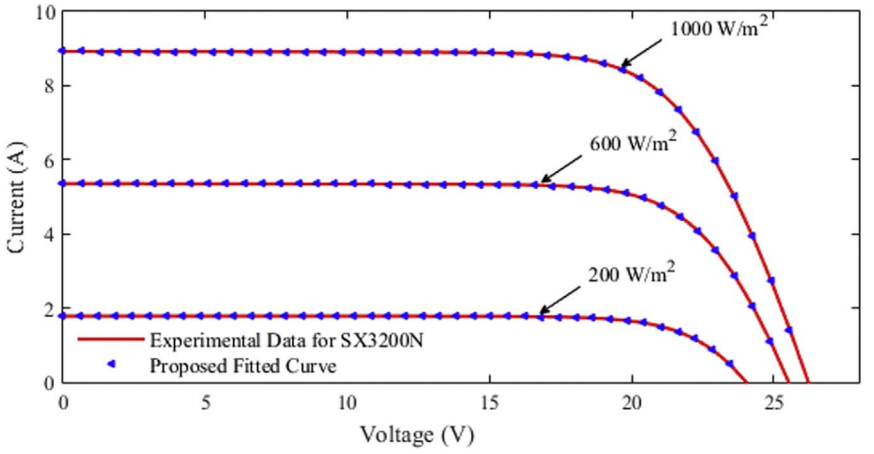

(b)

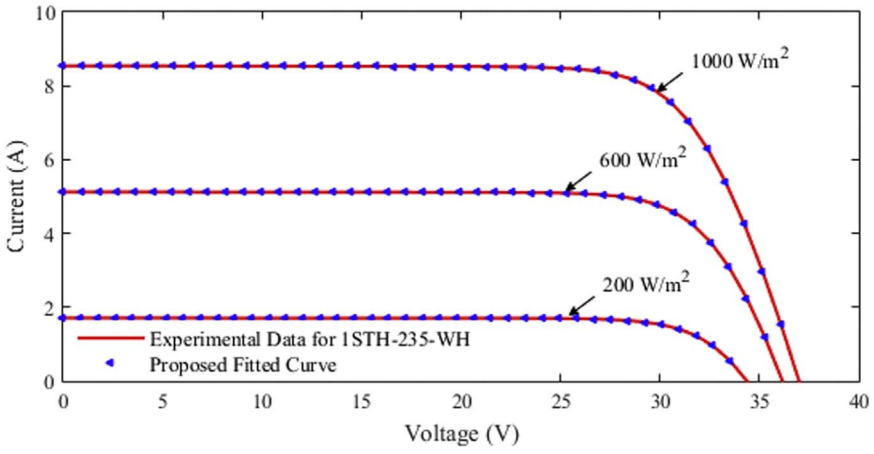

(c)

Fig. 19. Experimental and estimated characteristics at different irradiance levels: (a) KC200GT (b) SX3200N (c) 1STH-235-WH.

different irradiances were regenerated and compared with the experimental data for observing the accuracy of modeling. The comparison is illustrated in Fig. 19(a) for M/S Kyocera module, Fig. 19(b) for M/S BP Solar module and Fig. 19(c) for M/S 1Soltech module. It can be clearly inferred from Fig. 19 that the estimated characteristic curves are closely tracing the experimental curves for the considered three irradiation levels and over the entire range of data. Based on these investigations, it can be concluded that ER-WCA technique is able to effectively extract the parameters of PV modules even at the low irradiation values which is important during module operation under mismatch conditions, like partial shading.

5. Conclusion

In this work, Evaporation Rate based Water Cycle Algorithm (ER-WCA) has been explored for effective parameter estimation of PV

systems. Single and double diode based models of PV cell and single diode based model of PV module have been successfully identified from their respective single non-linear I-V characteristics. Modeling performance of ER-WCA was assessed in terms of root mean square error, mean absolute error and mean relative error, between computed and experimental data and it is found to be superior to the several recent potential published works, proving its practical effectiveness. Furthermore, modeling capability of ER-WCA was also investigated under varying temperature and irradiation conditions which further validated its suitability and effectiveness. Based on the presented detailed investigation it is concluded that ER-WCA is a promising optimization technique for PV cell/module identification.

References

[1] Solar Generation IV | Greenpeace International Report: ⟨http://www.greenpeace.org/sweden/Global/sweden/p2/klimat/report/2006/solar-generation-3rd-edition-2.pdf⟩. Accessed on: 20 June 2016.

[2] Renewables. Global status report: ⟨http://www.ren21.net/GSR-2016-Report-Full-report-EN⟩; 2016. Accessed on: 20 June 2016.

[3] M. A. Green, High efficiency silicon solar cells, Seventh EC Photovoltaic Solar Energy Conference, Springer Netherlands, 1987.

[4] V.J. Chin, Z. Salam, K. Ishaque, Cell modeling and model parameters estimation techniques for photovoltaic simulator application: a review, Appl. Energy 154 (2015) 500–519.

[5] Z. Ouennoughi, M. Chegaar, A simpler method for extracting solar cell parameters using the conductance method, Solid-State Electron. 43 (11) (1999) 1985–1988.

[6] S.K. Datta, K. Mukhopadhyay, S. Bandopadhyay, H. Saha, An improved technique for the determination of solar cell parameters, Solid-State Electron. 35 (11) (1992) 1667–1673.

[7] El Tayyan, A. Ahmed, An approach to extract the parameters of solar cells from their illuminated IV curves using the Lambert W function, Turk. J. Phys. 39 (1) (2015) 1–15.

[8] Shu-xian Lun, Shuo Wang, Gui-hong Yang, Ting-ting Guo, A new explicit double-diode modeling method based on Lambert W-function for photovoltaic arrays, Sol. Energy 116 (2015) 69–82.

[9] B. Romero, G. del Pozo, B. Arredondo, Exact analytical solution of a two diode circuit model for organic solar cells showing S-shape using Lambert W-functions, Sol. Energy 86 (10) (2012) 3026–3029.

[10] M.G. Villalva, G.R. Gazoli, Ernesto Ruppert Filho, Comprehensive approach to modeling and simulation of photovoltaic arrays, IEEE Trans. Power Electron. 24 (5) (2009) 1198–1208.

[11] Ken-ichi Ishibashi, Yasuo Kimura, Michio Niwano, An extensively valid and stable method for derivation of all parameters of a solar cell from a single current-voltage characteristic, J. Appl. Phys. 103 (9) (2008) 094507.

[12] X.S. Yang, Nature-Inspired Optimization Algorithms, Elsevier, London, 2014.

[13] Joseph A. Jervase, Hadj Bourdoucen, Ali Al-Lawati, Solar cell parameter extraction using genetic algorithms, Meas. Sci. Technol. 12 (11) (2001) 1922.

[14] M. Zagrouba, A. Sellami, M. Bouaïcha, M. Ksouri, Identification of PV solar cells and modules parameters using the genetic algorithms: application to maximum power extraction, Sol. Energy 84 (5) (2010) 860–866.

[15] Meiying Ye, Xiaodong Wang, Yousheng Xu, Parameter extraction of solar cells using particle swarm optimization, J. Appl. Phys. 105 (9) (2009) 094502.

[16] H. Wei, J. Cong, X. Lingyun, Extracting solar cell model parameters based on chaos particle swarm algorithm, in: Proceedings of the IEEE 2011 International Conference on Electric Information and Control Engineering (ICEICE), 2011.

[17] K. Ishaque, Zainal Salam, An improved modeling method to determine the model parameters of photovoltaic (PV) modules using differential evolution (DE), Sol. Energy 85 (9) (2011) 2349–2359.

[18] K. Ishaque, Zainal Salam, Saad Mekhilef, Amir Shamsudin, Parameter extraction of solar photovoltaic modules using penalty-based differential evolution, Appl. Energy 99 (2012) 297–308.

[19] Lian Lian Jiang, Douglas L. Maskell, Jagdish C. Patra, Parameter estimation of solar cells and modules using an improved adaptive differential evolution algorithm, Appl. Energy 112 (2013) 185–193.

[20] K.M. El-Naggar, M.R. AlRashidi, M.F. AlHajri, A.K. Al-Othman, Simulated annealing algorithm for photovoltaic parameters identification, Sol. Energy 86 (1) (2012) 266–274.

[21] M.F. AlHajri, K.M. El-Naggar, M.R. AlRashidi, A.K. Al-Othman, Optimal extraction of solar cell parameters using pattern search, Renew. Energy 44 (2012) 238–245.

[22] A. Askarzadeh, A. Rezazadeh, Parameter identification for solar cell models using harmony search-based algorithms, Sol. Energy 86 (11) (2012) 3241–3249.

[23] Jieming Ma, T.O. Ting, Ka Lok Man, Nan Zhang, Sheng-Uei Guan, Prudence W.H. Wong, Parameter estimation of photovoltaic models via cuckoo search, J. Appl. Math. (2013).

[24] Diego Oliva, Erik Cuevas, Gonzalo Pajares, Parameter identification of solar cells using artificial bee colony optimization, Energy 72 (2014) 93–102.

[25] Qun Niu, Letian Zhang, Kang Li, A biogeography-based optimization algorithm with mutation strategies for model parameter estimation of solar and fuel cells, Energy Convers. Manag. 86 (2014) 1173–1185.

[26] Lei Guo, Zhuo Meng, Yize Sun, Libiao Wang, Parameter identification and sensitivity analysis of solar cell models with cat swarm optimization algorithm, Energy Convers. Manag. 108 (2016) 520–528.

[27] M. Jamadi, Farshad Merrikh-Bayat, Mehdi Bigdeli, Very accurate parameter estimation of single-and double-diode solar cell models using a modified artificial bee colony algorithm, Int. J. Energy Environ. Eng. 7 (1) (2016) 13–25.

[28] Xu Chen, Kunjie Yu, Wenli Du, Wenxiang Zhao, Guohai Liu, Parameters identification of solar cell models using generalized oppositional teaching learning based optimization, Energy 99 (2016) 170–180.

[29] N.F.A. Hamid, Nasrudin Abd Rahim, Jeyraj Selvaraj, Solar cell parameters identification using hybrid Nelder-Mead and modified particle swarm optimization, J. Renew. Sustain. Energy 8 (1) (2016) 015502.

[30] Ali Sadollah, Hadi Eskandar, Ardeshir Bahreininejad, Joong Hoon Kim, Water cycle algorithm with evaporation rate for solving constrained and unconstrained optimization problems, Appl. Soft Comput. 30 (2015) 58–71.

[31] Hadi Eskandar, Ali Sadollah, Ardeshir Bahreininejad, Mohd Hamdi, Water cycle algorithm–a novel metaheuristic optimization method for solving constrained engineering optimization problems, Comput. Struct. *110* (2012) 151–166.

[32] D.S.H. Chan, J.R. Phillips, J.C.H. Phang, A comparative study of extraction methods for solar cell model parameters, Solid-State Electron. 29 (3) (1986) 329–337.

[33] M. Wolf, Hans Rauschenbach, Series resistance effects on solar cell measurements, Adv. Energy Convers. 3 (2) (1963) 455–479.

[34] T. Easwarakhanthan, J. Bottin, I. Bouhouch, C. Boutrit, Nonlinear minimization algorithm for determining the solar cell parameters with microcomputers, Int. J. Sol. Energy 4 (1) (1986) 1–12.

[35] System Advisor Model, SAM 2014.1.14: General Description - NREL : ⟨www.nrel.gov/docs/fy14osti/61019.pdf⟩. Accessed on: 20 June 2016.

[36] J.A. Duffie, William A. Beckman, Solar Engineering of Thermal Processes 3, Wiley, New York, 2013.

[37] G. Musser, Solar at Home: invert your thinking: squeezing more power out of your solar panels, Sci. Am. 26 (3) (2009).

[38] P.G. Charalambous, G.G. Maidment, S.A. Kalogirou, K. Yiakoumetti, Photovoltaic thermal (PV/T) collectors: a review, Appl. Therm. Eng. 27 (2) (2007) 275–286.